

Capacitor Placement in Distorted Distribution Network Subject to Wind and Load Uncertainty

A. Najafi, R. Aboli, H. Falaghi*, M. Ramezani

Department of Electrical and Computer Engineering, University of Birjand, Birjand, Iran

Abstract- Utilizing capacitor banks is very conventional in distribution network in order for local compensation of reactive power. This will be more important considering uncertainties including wind generation and loads uncertainty. Harmonics and non-linear loads are other challenges in power system which complicates the capacitor placement problem. Thus, uncertainty and network harmonics have been considered in this paper, simultaneously. Capacitor placement has been proposed as a probabilistic harmonic problem with different objectives and technical constraints in the capacitor placement problem. Minimizing power and energy loss and capacitor prices are considered as objectives. Particle Swarm Optimization (PSO) and Differential Evolution (DE) algorithms have been used to solve the optimization problem. Loads are subjected to uncertainty with normal probabilistic distribution function (PDF). Auto Regressive and Moving Average (ARMA) time series and two point estimate method have also been utilized to simulate the wind speed and to perform the probabilistic load flow, respectively. Finally, the proposed method has been implemented on standard distorted test cases in different scenarios. Monte Carlo Simulation (MCS) has also been used to verify the probabilistic harmonic power flow. Simulation results demonstrate the efficiency of the proposed method.

Keyword: Uncertainty, Two point estimate method, Probabilistic harmonic power flow, PSO, DEA.

1. INTRODUCTION

1.1 Problem description and literature review

Flowing reactive current in the network causes decreasing transmission capability and increasing losses. Therefore, capacitor banks are installed in the distribution network in order to decrease losses and harmonics harmful effects and to improve voltage quality [1]. There is a great attention to decrease the harmonics with increasing non-linear loads. As result, capacitor placement, as a way to decrease harmonics, has attracted researchers' concentrations [2]. A joint optimization algorithm has been suggested in Ref. [3] for replacement of conductor and placement of capacitors in order to reduce the power and energy loss in the network. Differential evolution and pattern search (DE-PS) have been used as meta-heuristic optimization tools to solve optimal capacitor placement problem in Ref. [4]. To tackle and reduce the search

space process and computational CPU time, the potential buses candidate for capacitor allocations have been pre-identified. In Ref. [5] a dynamic model considering multi-period capacitor allocation problem of primary radial distribution system is proposed in order to maintain the voltage profile. An evolutionary method has been suggested in Ref. [6] for optimal capacitor placement in large test systems. Authors in Refs. [7,8] and [9] have investigated the methods to reduce voltage and current harmonics. Optimization methods are used in order to determine optimal size and location of the capacitors in the distribution network. In Ref. [10] a mixed integer programming (MIP) method has been proposed to solve capacitor placement problem which has considered voltage and power constraints simultaneously and the problem has been divided to main and sub problem. MIP has also been used in Refs. [11,12] optimal capacitor placement in distribution transformers in order to decrease the power loss. The capacitors have been installed in low voltage side of transformers. Some papers have indicated candidate buses for placement before solving main problem [13]. Authors in Ref. [14] have investigated the capacitor placement and reconfiguration problem, simultaneously. In Ref. [15] a hybrid optimization algorithm has been suggested for the optimal placement of shunt capacitor

Received: 13 July 2015

Revised: 13 Oct. 2015 and 8 Apr. 2016

Accepted: 12 June 2016

*Corresponding author:

E-mail: falaghi@birjand.ac.ir (H. Falaghi)

banks in radial distribution networks in the presence of different voltage-dependent load models. Utilizing evolutionary methods have been increased in recent years in order to capacitor placement. Application of Genetic Algorithm (GA) has shown in Ref. [16]. In Refs. [17], [18] and [19] Immune System Algorithm (ISA), Differential Evolution (DE) and Cuckoo Search Algorithm (CSA) have been suggested, respectively. In Refs. [20] and [21] fuzzy methods have also been used. Each of the mentioned papers has considered different objective. For example, Ref. [1] has considered loss and cost as objectives and Ref. [22] has solved the problem in multi objective framework. Increasing energy requirement and decreasing fossil fuel lead mankind to utilize the renewable energies [23]. Due to the economic and environmental effects, wind power has penetrated in the power system. Installing wind turbines have been increased in distribution networks in recent years. Wind power has probabilistic nature which increases complexity of the related problems. Also, considering load uncertainties in the problem causes changing optimum solution.

1.2. Paper contribution

The main contribution of this paper is to determine the optimal size of capacitors, considering wind turbines and load uncertainties in a distorted distribution network. The sources of uncertainties are parametric and dynamic uncertainty of wind speeds are eliminated using multi-generation levels for wind turbine. Probabilistic Harmonic Power Flow (PHPF) is used in order to perform power flow in probabilistic and harmonic environment. Point estimate method is utilized to give the capability of probability to the harmonic power flow. This method has been used in different papers and its capability has been demonstrated in Refs. [24,25]. PSO and DE have also been utilized in order to solve the problem as an optimization tool. Simulations are conducted on 18 and 30 buses standard distorted test case. Peak load level and three load levels are considered during optimization process. Finally, a comparison is done with MCS and the capability of PHPF is verified. It should be noted that MCS is only used to verify the PHPF results and it hasn't been used in the optimization process. Main contributions of the paper are listed briefly, as follows:

- Considering the wind speed probability in the capacitor placement problem with multi-generation levels for the wind turbines generation.
- Considering the nonlinear loads and wind turbines harmonic and using the capacitors set to decrease the Total Harmonic Distortion (THD).
- Considering the uncertainty and nonlinearity of the loads, simultaneously.
- Using a probabilistic harmonic power flow in the capacitor placement problem to perform load flow in the uncertainty and harmonic environments.

1.3. Paper organization

The paper is organized as follows: problem formulation is proposed in the next section then, wind power modeling is presented, following it, power flow method is described and then, particle swarm optimization algorithm is described. After that, numerical result is proposed and finally, conclusion is given.

2. WIND POWER OUTPUT MODELING

2.1. Wind speed modeling

The hourly mean and standard deviation of the wind speeds from a 10-year database (from 1st January 2000 to 31st December 2010) for the Mandan location were obtained from Environment North Dakota. The average and standard deviation of the wind speed are 9.98 m/s and 4.84, respectively. These data have been used to make Auto-Regressive and Moving Average (ARMA) time series model [26,27]. The ARMA time series is expressed mathematically as follows:

$$z_t = \varepsilon_t + \sum_{i=1}^m \psi_i z_{t-1} + \sum_{j=1}^n \theta_j \varepsilon_{t-j} \quad (1)$$

Where z_t is the time series value at time t , $\psi_i (i = 1, 2, 3, \dots, m)$ and $\theta_j (j = 1, 2, 3, \dots, n)$ are auto regressive and moving respectively. ε_t is normal white noise. Simulated wind speed at hour t (WS_t) is calculated as below:

$$WS_t = \mu_t + \sigma_t \cdot z_t \quad (2)$$

Where μ_t and σ_t are historical mean and standard deviation of wind speed at hour t .

2.2. Wind power output

Relation of wind turbine output power and speed is expressed by Eq. (3) [28]. There are three main parameters in it, V_n , V_{cin} and V_{cout} . It is visible that when the speed reaches to V_{cin} , turbine starts to generate power and when speed reaches to V_n output power will fix on P_n . The turbine will also stop the power generation if the speed gets to V_{cout} . V_{cin} , V_{cout} and V_n are 3.5, 25 and 10.5 m/s, respectively. Mathematical equations are as follows:

$$P_t = \begin{cases} 0 & 0 \leq WS_t \leq V_{cin} \\ A + B \times WS_t + C \times WS_t^2 & V_{cin} \leq WS_t \leq V_n \\ P_n & V_n \leq WS_t \leq V_{cout} \\ 0 & V_{cout} \leq WS_t \end{cases} \quad (3)$$

where P_t and WS_t are wind power output and wind speed at hour t , respectively. Coefficients A , B and C are constant values and they are obtained by V_n , V_{cin} and V_{cout} . Their equations are available in Ref. [29].

2.3. Power output modeling

Simulations are done for 8760 hours, therefore there are 8760 speeds. Different speeds are concluded to different power outputs. For the sake of simplicity, power output is approximated with a piecewise curve with specific steps. Increasing in steps number leads to more computational time and more accuracy. So, a tradeoff should be created between accuracy and computational time. Each step is described by its value and probability. The probability of i th step (p_{si}) is calculated as follows:

$$p_{si} = \frac{N_i}{8760} \quad (4)$$

where N_i is the number of simulated wind speed in i th step. Fig. 1 shows a sample approximating with six steps. Vertical axis is the produced power by the wind turbine and horizontal axis is the time duration. Continuous line shows the real output of the wind turbine and dash line depicts its approximation. Each step probability of the dash line is determined by Eq. (4).

3. PROBLEM FORMULATION

Optimal capacitor placement problem has various variables and parameters such as capacitor sizes. Moreover, there are constraints like voltage magnitude and maximum allowable harmonic value. Objectives and constraints are as follows:

Table 1 also illustrates each step production with related probabilities.

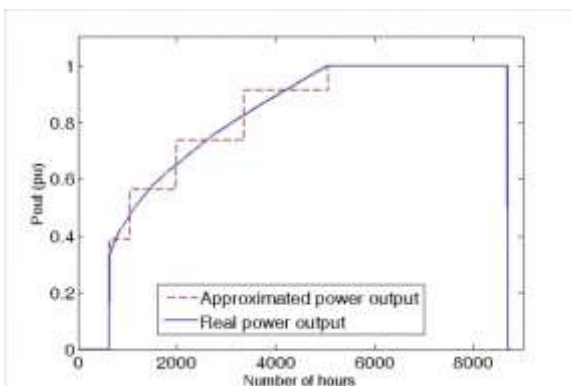


Fig. 1. A sample wind generation approximating with six steps

3. PROBLEM FORMULATION

Optimal capacitor placement problem has various variables and parameters such as capacitor sizes. Moreover, there are constraints like voltage magnitude and maximum allowable harmonic value. Objectives and constraints are as follows:

Table 1. Production and related probabilities for sample approximating with six steps

Wind power generation states (pu)	Probability
0	0.08071
0.300	0.04715
0.475	0.10719
0.650	0.15616
0.825	0.19452
1	0.41427

3.1. Objective function

Different objectives are considered in the capacitor placement problem. In this paper, objective is minimizing the expected value of the power and energy loss and capacitor prices. It is shown mathematically as follows:

$$E \text{ Cost} = \sum_{i=1}^{ns} k_p EP_{loss}^i + \sum_{j=1}^{nc} k_c \cdot EQ_c^j + \sum_{l=1}^L \sum_{t=1}^T K_e \cdot t \cdot EP_{loss}^l \quad (5)$$

where $E \text{ Cost}$ is expected value of the total cost, EP_{loss}^i is the expected value of loss in section i , ns is number of the sections, EQ_c^j and EP_{loss}^l are expected values of the capacitor prices and losses in load level l , respectively. nc , k_p , k_c , k_e and T are also number of the capacitors, saving per megawatt for loss reduction, cost per unit of fixed capacitance, cost per megawatt-hour and duration of load level l , respectively.

When generation uncertainties are considered, Eq. (5) is changed as follows:

$$E \text{ Cost} = \sum_{g=1}^G p_g \cdot (\sum_{i=1}^{nb} k_p EP_{loss}^i + \sum_{j=1}^{nc} k_c \cdot EQ_c^j + \sum_{l=1}^L \sum_{t=1}^T K_e \cdot t \cdot EP_{loss}^l) \quad (6)$$

Where, p_g is the probability of generation level g , G is total number of generation levels.

3.2. Constraints

The expected value of voltage magnitude mustn't violate its upper and lower bounds. It is described mathematically as follows [2]:

$$V_{min} \leq EV_i \leq V_{max} \quad (7)$$

where, EV_i is expected value of the bus voltage i , V_{\min} and V_{\max} are upper and lower bounds of the voltage and considered to be 0.95 and 1.05, respectively.

The maximum expected value of allowable harmonic in the system ($ETHD$) is another constraint which is considered in the paper. A standard amount is considered for maximum system Total Harmonic Distortion (THD^{\max}). This constraint is as follows:

$$ETHD \leq THD^{\max} \quad (8)$$

4. POWER FLOW

4.1. Harmonic power flow

Harmonic Power Flow (HPF) is used to analyze the systems with non-linear loads. HPF has differences with classic power flow. Active and reactive power equations are only considered in base frequency in classic power flow while, harmonic power flow requires more equations to analyze the system in different frequencies. Multiple methods have been suggested to perform harmonic power flow. For example, [30,31] have described Newton-Raphson method. In this paper, HPF has been conducted with DigSilent software which uses Newton-Raphson method [32].

4.2. Probabilistic harmonic power flow

Deterministic harmonic load flow was described in previous section, briefly. But, power system has probabilistic nature and its inputs vary in their intervals. Thus, it can't be used deterministic methods to evaluate the probabilistic problems. Probabilistic harmonic power flow is used for the problems with probabilistic inputs.

In Refs. [33,34] the methods have been suggested to perform probabilistic harmonic power flow. They have used point estimate method to run probabilistic harmonic power flow. This method is very simple and it has accuracy and speed. Ref. [24] has utilized the point estimate method to solve the optimal power flow problem considering uncertainties. Efficiency of these references is also verified by comparing with MCS. Point estimate method is described as follows.

It is assumed that harmonic power flow equations are as follows:

$$X = G(p_1, p_2, \dots, p_l, \dots, p_m) \quad (9)$$

where, X is state variable vector (base frequency and harmonic frequencies voltage), G is harmonic power flow equations and p_l is l th probabilistic input.

It is assumed that each of the probabilistic inputs has apparent average and standard deviation in point estimate method. First, one of the probabilistic inputs is

selected and then, two estimates are calculated by Eq. (10).

$$p_{l,k} = \mu_{p_l} + \zeta_{l,k} \sigma_{p_l} \quad , \quad k=1,2 \quad (10)$$

where, μ_{p_l} and σ_{p_l} are average and standard deviation of input p_l , respectively. In Eq. (10), standard location $\zeta_{l,k}$ is calculated by Eq. (11).

$$\zeta_{l,k} = \lambda_{l,3}/2 + (-1)^{3-k} \sqrt{m + (\lambda_{l,3}/2)^2} \quad (11)$$

where, m is number of probabilistic inputs and $\lambda_{l,3}$ is coefficient of skewness and it is described as follows:

$$\lambda_{l,3} = E\left[\left(p_l - \mu_{p_l}\right)^3\right] / \sigma_{p_l}^3 \quad (12)$$

By calculating two estimates $p_{l,1}$ and $p_{l,2}$ for input p_l and placing in Eq. (13), two estimates ($X_{l,1}$, $X_{l,2}$) are made as follows:

$$X_i(l,k) = G(\mu_{p_1}, \mu_{p_2}, \dots, p_{l,k}, \dots, \mu_{p_m}) \quad , \quad k=1,2 \quad (13)$$

Two points are estimated for each state up to this step. Therefore, if there were m probabilistic inputs, then, $2m$ estimate would be available.

j th moment of X_i is calculated by Eq. (14).

$$E(X_i^j) \cong \sum_{l=1}^m \sum_{k=1}^2 \omega_{l,k} [X_i(l,k)]^j \quad (14)$$

where $\omega_{l,k}$ is weighting factor for $X_i(l,k)$ and it is shown as Eq. (15).

$$\omega_{l,k} = \frac{1}{m} (-1)^k \frac{\zeta_{l,3-k}}{\zeta_l} \quad , \quad k=1,2 \quad (15)$$

Finally, average and standard deviation of i th state variable is proposed by Eqs. (16) and (17).

$$\mu_{X_i} = E(X_i) \quad (16)$$

$$\sigma_{X_i} = \sqrt{E(X_i^2) - [E(X_i)]^2} \quad (17)$$

It is noticeable that if coefficient of skewness is zero, Eqs. (11) and (15) will be constant values for all of the probabilistic inputs which are related to number of probabilistic inputs.

Figure 2 shows the probabilistic harmonic power flow flowchart.

5. OPTIMIZATION ALGORITHMS

5.1. Particle swarm optimization

Each particle in PSO is a candidate solution in multidimensional space of the problem. Candidate solutions have two main parts, current position (P_i) and current velocity (V_i), which are expressed by [35]:

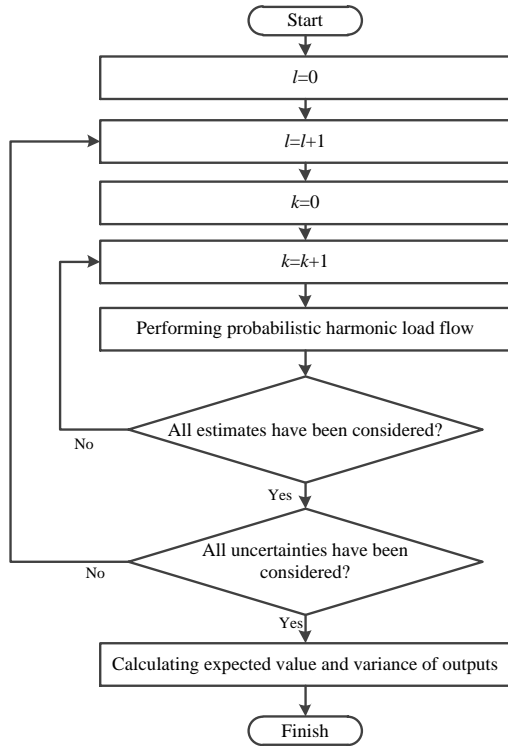


Fig. 2. Flowchart of implementing probabilistic harmonic power flow

$$P_i = (p_i^1, p_i^2, \dots, p_i^{ns}) \quad (18)$$

$$V_i = (v_i^1, v_i^2, \dots, v_i^{ns})$$

where, ns is the dimension of the problem and i is the iteration index. The new position of each particle is created by its current position and new velocity. New velocity is produced by four factors, the current velocity and position, the particle's best position ($PBest$), and the best position among all of particles in all iterations ($GBest$). Therefore, new velocity is obtained as follows:

$$V_{i+1} = \omega V_i + r_1 \cdot (PBest_i - P_i) + r_2 \cdot (GBest - P_i) \quad (19)$$

where, ω is the particle inertia coefficient, r_1 and r_2 are random numbers between 0 and 1, respectively. The new position of the particle is obtained by:

$$P_{i+1} = P_i + V_{i+1} \quad (20)$$

The process is continued until convergence criteria are met.

5.2. Differential evolution algorithm

DE includes three main operators, namely, mutation, crossover, and selection. Also, it has three control parameter, namely, population size (np), scaling coefficient (F), and crossover probability (CR) [36]. In an n -dimensional search space, the structure of member

k is represented as vector $X_k = (x_{k,1}, x_{k,2}, \dots, x_{k,n})$ where the dimension represents the number of

components. In the first stage of the DE optimization process, initial population contains np members should be created randomly. After the population is initialized, the operators of mutation, crossover and selection create the population of the next generation. At the generation t , the process for creation of a mutant solution (Y_k) for each parent (X_k) in the population can be expressed as follows:

$$Y_k(t) = X_{r3}(t) + F \cdot (X_{r1}(t) - X_{r2}(t)), \quad k=1, 2, \dots, np \quad (21)$$

where vector indices $r1$, $r2$, and $r3$ are randomly chosen, which $r1$, $r2$, and $r3 \in \{1, \dots, np\}$ and $r1 \neq r2 \neq r3 \neq k$. X_{r1} , X_{r2} , and X_{r3} are selected members for each parent vector. F is a user-defined constant known as the 'scaling factor', which is a positive and real number. The usual choice for F is a number between 0 and 1. At the generation t , the crossover operator creates a new solution (child) (Z_k) using each parent (X_k) and its related mutant vectors (Y_k) as follows:

$$z_{kj}(t) = \begin{cases} y_{kj}(t) & \text{if } rand \leq CR \\ & \text{or } j = jrand, \text{ for } j = 1, \dots, n \\ x_{kj}(t) & \text{otherwise} \end{cases} \quad (22)$$

where, CR is 'crossover probability' which is selected within the range $[0, 1]$. $rand$ is a uniformly distributed random number within the range $(0,1)$ generated a new for each component j . Here, $jrand \in [1, 2, \dots, n]$ and ensures that the trial vector gets at least one parameter from the mutant vector. The selection operator compares the fitness of the parent and the corresponding child and the fitter of the two solutions is then allowed to advance into the next generation. The selection process can be expressed as:

$$X_k(t+1) = \begin{cases} Z_k(t) & FIT(X_k(t)) \geq FIT(Z_k(t)) \\ X_k(t) & \text{otherwise} \end{cases} \quad (23)$$

where, $FIT(\cdot)$ is the fitness function.

5.3. Optimizing process

Each solution contains the capacitors set in DE or PSO algorithm. DPL environment of DigSilent software is used in order to optimize the problem and penalizing method is utilized to satisfy the inequality constraints. Two inequality constraints are the allowable values of the voltage and THD. To handle these constraints a penalty term is used such a way infeasible solutions are penalized as follows:

$$Penalty = PF \cdot |A - \bar{A}| \quad (24)$$

where, A is voltage or THD and \bar{A} is their bounds and PF is a constant positive number.

Then, objective function f is updated as follows:

$$f = f + Penalty \tag{25}$$

Figure 3 shows the flowchart of optimization process.

6. NUMERICAL RESULTS

Simulations are conducted on a computer Ci5, 4GByte RAM by DigSilent software on two test cases. Number of iterations and population are 60 and populations are 50 for 18 bus test case and 70 and 40 for 30-bus test case to perform PSO and DE algorithms. Simulations are done in four scenarios. In the first scenario, wind generation has uncertainty and turbines don't produce harmonic and loads are deterministic.

The second scenario is similar to first scenario with a difference in which, wind turbines produce harmonic. Load uncertainties have also been considered in the third scenario. For the fourth scenario more harmonic sources are considered. It should be noted that the first, second and third scenarios are conducted on 18- bus test case with one load level and the fourth scenario is conducted on the 30-bus test case with three load levels. Finally, a sensitivity analysis has been done on the wind turbines generation levels to investigate its accuracy in 18-bus test system.

6.1. Test systems

- *18-bus test case*

This case is a standard harmonic test case. (See Figure 4) [37]. Capacitors cost is selected from [38]. This case is a distorted case and its initial THD is 8.48%, which is upper than the standard value. Total initial loss, minimum and maximum voltages are 280 kw, 0.947 and 0.999 pu, respectively. The capacitors places are fixed which are visible in the figure. Three wind turbines are added to test case in buses 8, 9 and 24. Maximum active capacity of turbines is 1000 Kw and maximum reactive capacity is 250 KVar. Wind turbines generations are approximated with six steps for modeling uncertainties same as Table 1. Bus 6 has a non-linear load which causes harmonic in the network.

- *30-bus test case*

A test case with 30 buses is selected in order to more investigate the PHPF with three levels of loads (see Figure 5). The test case data including line data, branches data, initial capacitors set and harmonics data are available in Ref. [39]. Seven capacitors are in bus 1, 14, 16, 20, 24 and 26. Total initial loss with and without initial capacitors set are 440 and 530 kw, respectively and the amount of THD is 11.54% with initial capacitors set. Three wind turbines are also considered in bus 22, 28 and 30 without considering the harmonics.

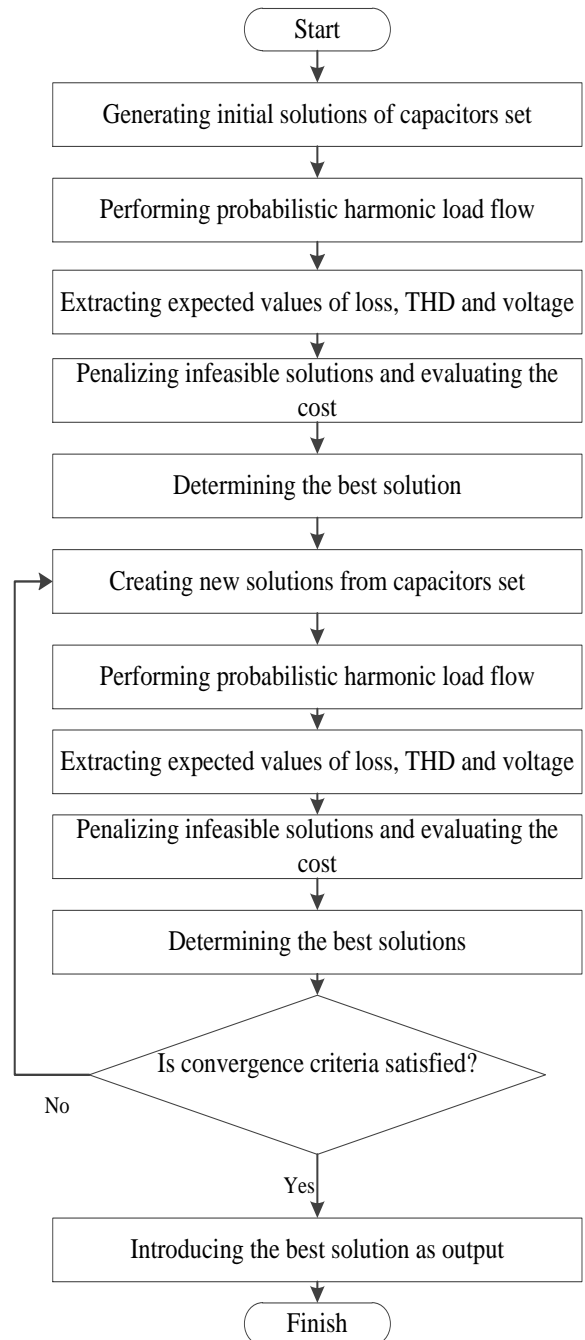


Fig. 3. Flowchart of optimizing process

6.2. The first scenario

Generation uncertainties are considered in this scenario and loads are deterministic. Simulation results including: Expected amount of network loss, cost and optimal set of capacitors have been listed in Tables 2-4 for DE and PSO algorithms. Using wind generation as a distributed generation system has decreased the network loss. Results demonstrate feasibility of the solution. It is because expected value of the maximum and minimum voltage and the maximum allowable THD are in range while the loss and cost are decreased. Also, DE and PSO closest results are verified each other results.

Table 2. Simulation results by PSO in the first scenario

Index	Expected Value	Index	Expected Value
THD (%)	4.96	Injected reactive power (MVar)	10.2
Maximum voltage (pu)	1.010	Energy losses (MWh)	1564.07
Minimum voltage (pu)	0.972	Capacitor cost (\$/year)	2128
Power losses (MW)	0.17962	Total cost (\$/year)	102066.3

6.3. The second scenario

This scenario is same as previous scenario but wind turbine harmonic has also been considered. Harmonics in different frequencies are available in Ref. [40] and Table 5.

Main contribution of this scenario is achieving to the best solution by thwarting wind harmonics with the capacitors. It means, optimal solution is only found by changing the capacitors reactive power generation. Simulation results have been listed in Tables 5-7 which demonstrate the efficiency of proposed method in both DE and PSO algorithms. Results in Table 8 are similar to previous scenario while generated reactive powers are different from previous scenario. Actually, similar results are found by frustrating wind turbines harmonics by changing capacitor set generations.

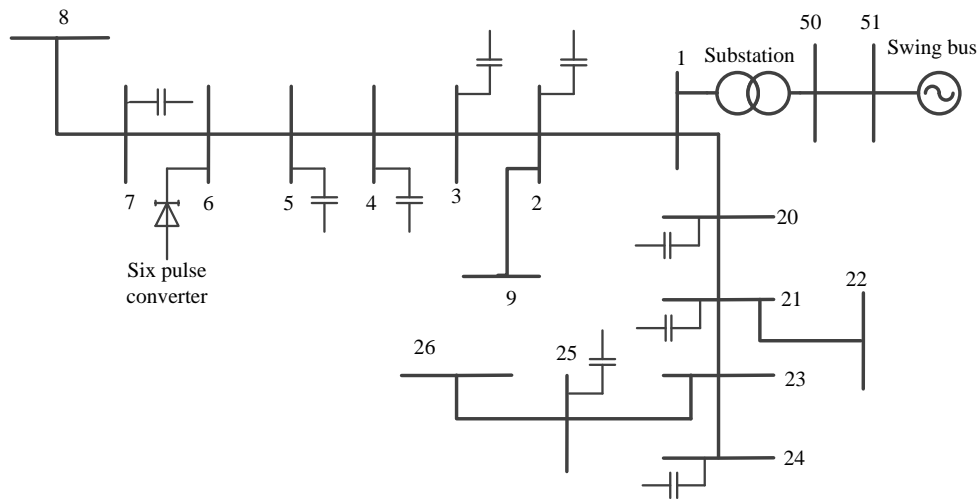


Fig. 4. 18 buses distorted test case

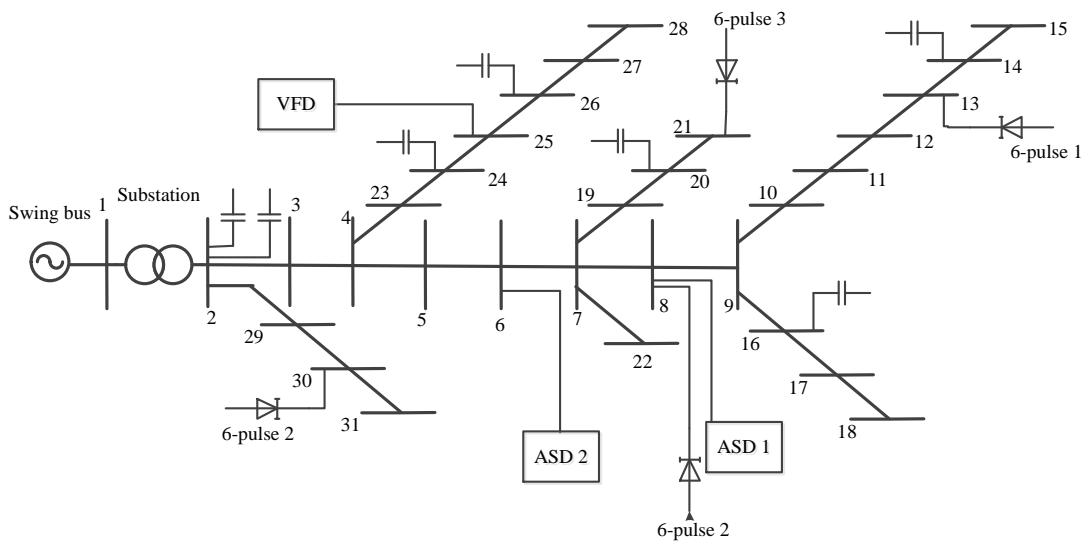


Fig. 5. 30 buses distorted test case

Table 3. Simulation results by DE in the first scenario

Index	Expected Value	Index	Expected Value
THD (%)	4.963779	Injected reactive power (MVar)	10.05
Maximum voltage (pu)	1.01467	Energy losses (MWh)	1569.8
Minimum voltage (pu)	0.976893	Capacitor cost (\$/year)	2040.75
Power losses (MW)	0.17927	Total cost (\$/year)	102043.2

Table 4. Optimal capacitor set in the first scenario

Reactive power		Q ₂	Q ₃	Q ₄	Q ₅	Q ₇
Size (MVar)	PSO	0.15	0.3	3.15	3.15	0.3
	DE	0.3	0	3	2.1	1.35
Reactive power		Q ₂₀	Q ₂₁	Q ₂₄	Q ₂₅	Q ₅₀
Size (MVar)	PSO	1.2	0.6	0	0.45	0.9
	DE	0.45	0.15	0	1.65	1.05

Table 5. Percent of harmonics in different orders

Order	Magnitude (%)	Order	Magnitude (%)
5	4	29	0.6
7	4	31	0.6
11	2	35	0.3
13	2	37	0.3
17	1.5	41	0.3
19	1.5	43	0.3
23	0.6	47	0.3
25	0.6	49	0.3

Table 6. Simulation results by PSO in the second scenario

Index	Expected Value	Index	Expected Value
THD (%)	4.961145	Injected reactive power (MVar)	10.2
Maximum voltage (pu)	1.017602	Energy losses (MWh)	1571.73
Minimum voltage (pu)	0.981334	Capacitor cost (\$/year)	2011.95
Power losses (MW)	0.17933	Total cost (\$/year)	102118

Table 7. Simulation results by DE in the second scenario

Index	Expected Value	Index	Expected Value
THD (%)	4.999271	Injected reactive power (MVar)	9.75
Maximum voltage (pu)	1.013579	Energy losses (MWh)	1560
Minimum voltage (pu)	0.974682	Capacitor cost (\$/year)	2131.05
Power losses (MW)	0.178082	Total cost (\$/year)	101500.9

Table 8. Optimal capacitors set in the second scenario

Reactive power		Q ₂	Q ₃	Q ₄	Q ₅	Q ₇
Size	PSO	0.9	1.2	3.15	2.4	0.15
	DE	1.05	0	2.85	1.5	0.3
Reactive power		Q ₂₀	Q ₂₁	Q ₂₄	Q ₂₅	Q ₅₀
Size	PSO	1.2	0.6	0.3	0.3	0
	DE	0.3	0.15	0.75	0.75	2.1

6.4. The third scenario

Generation and load uncertainties are considered in this scenario. Wind turbines also generate harmonic. Loads are modeled by normal distribution function. Loads average is equal with their available amount by considering 10 % standard deviation. PHPF is used to perform power flow in this scenario and the results including expected values and standard deviations (Std) are available in Table 9 and 10 for PSO and DE algorithms, respectively. The results of two algorithms are very close which shows the truthiness of two algorithms result. It is obvious that expected values of the constraints are in their bounds. Table 11 also shows the best combination of the capacitors resulted by PSO algorithm. MCS is implemented in order to validate the results of PHPF. For this aim, after finishing the optimization process, the best obtained solution by PSO algorithm is placed in the network and then MCS harmonic load flow is run. Results are demonstrated in Figs. (6) to (9), graphically. The results of two methods are closed which verify efficiency of PHPF. MCS demonstrates that, the outputs have a model similar to the normal probability distribution function like the inputs with a nuance difference with the normal PDF.

6.5. The fourth scenario: 30-bus test case

A larger test case is considered in order to illustrate the efficiency of the proposed model. The loads have three levels including 500 hour in peak load, 5000 hour in medium load and 3260 hours in off-peak load. The wind generations levels, the peak load loss and the energy loss coefficients and the capacitors cost are same as previous scenarios.

Table 9. Simulation results by PSO in the third scenario

Index	Expected Value	Std
THD (%)	4.936379	0.341166
Maximum voltage (pu)	1.0151	0.004455
Minimum voltage (pu)	0.976446	0.009239
Power losses (MW)	0.181095	0.017924
Index	Expected Value	
Injected reactive power (MVar)	9.9	
Energy losses (MWh)	1586.5	
Capacitor cost (\$/year)	2038.20	
Total cost (\$/year)	103001.2	

Simulations are conducted with PSO and DE algorithms in four states including; PSO algorithm with deterministic load, DE algorithm with deterministic loads, PSO algorithm with uncertain loads and PSO algorithm with uncertain loads.

Table 10. Simulation results by DE in the third scenario

Index	Expected Value	Std	Index	Expected Value
THD (%)	4.923804	0.355956	Injected reactive power (MVar)	11.25
Maximum voltage (pu)	1.017423	0.004738	Energy losses (MWh)	1567.6
Minimum voltage (pu)	0.980671	0.009211	Capacitor cost (\$/year)	2233.95
Power losses (MW)	0.178955	0.016745	Total cost (\$/year)	102090.8

Table 11. Optimal capacitors set in the third scenario

Reactive power		Q ₂	Q ₃	Q ₄	Q ₅	Q ₇
Size (MVar)	PSO	1.65	0.6	2.55	2.25	0.9
	DE	0.45	1.2	2.55	3.3	0.45
Reactive power		Q ₂₀	Q ₂₁	Q ₂₄	Q ₂₅	Q ₅₀
Size (MVar)	PSO	1.05	0.3	0.15	0.45	0
	DE	0.45	0.15	0.45	1.2	1.05

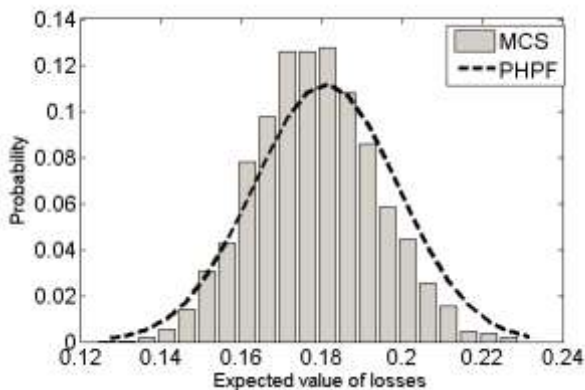


Fig. 6. Comparison of PHPF and MCS for the network loss

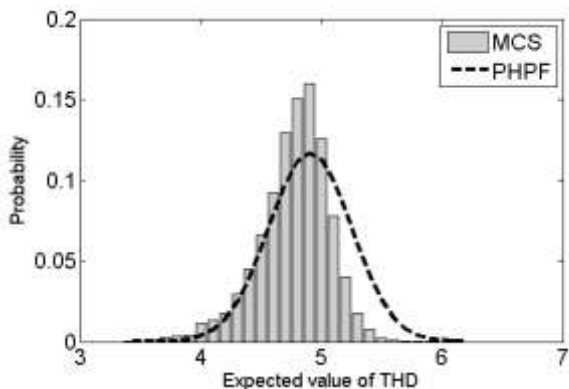


Fig. 7. Comparison of PHPF and MCS for the network THD

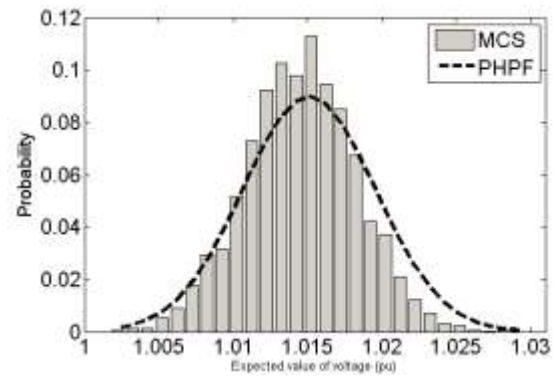


Fig. 8. Comparison of PHPF and MCS for the network maximum voltage

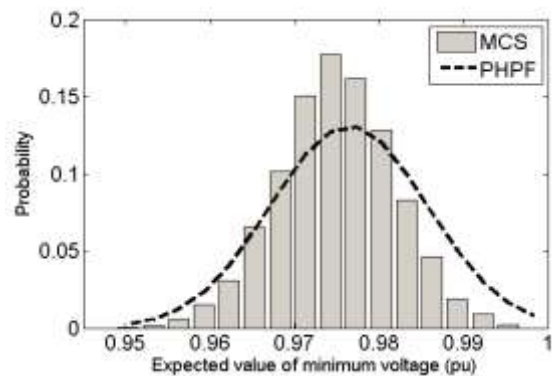


Fig. 9. Comparison of PHPF and MCS for the network minimum voltage

The results containing the capacitors optimal values, deterministic and the expected values of the outputs are summarized in table 12 to 16. Comparing the total cost of the deterministic state with uncertain state declares the increasing in the cost by considering the uncertainty. Furthermore, comparing the DE and PSO algorithm shows the close cost. The THD has been decreased to feasible bound from 11.54%.

Table 12. Simulation results in the 30-bus test case by PSO with deterministic loads

index	Value	index	Value
THD (%)	4.99	Injected reactive power (MVar)	6
Maximum voltage (pu)	1.05	Energy losses (MWh)	209.77
Minimum voltage (pu)	0.991	Capacitor cost (\$/year)	1190.85
Power losses (MW)	0.421	Total cost (\$/year)	62199.56

Optimal capacitors set for the four aforementioned states are summarized in Table 17. The uncertainty causes a change in capacitors set. Also, DE and PSO cost even though have nuanced difference, but their optimal capacitors set have very difference. Figure 10 depicts the convergence diagram in the four mentioned states.

Table 13. Simulation results in the 30-bus test case by DE with deterministic loads

index	Value	index	Value
THD (%)	4.90	Injected reactive power (MVar)	6
Maximum voltage (pu)	1.05	Energy losses (MWh)	213
Minimum voltage (pu)	0.9899	Capacitor cost (\$/year)	1282.05
Power losses (MW)	0.421	Total cost (\$/year)	62452.08

Table 14. Simulation results in the 30-bus test case by PSO with uncertain loads

index	Expected Value	Std	index	Expected Value
THD (%)	4.87	1.41	Injected reactive power (MVar)	5.4
Maximum voltage (pu)	1.05	2E-08	Energy losses (MWh)	222.83
Minimum voltage (pu)	0.992	0.01	Capacitor cost (\$/year)	1060.65
Power losses (MW)	0.444	0.0336	Total cost (\$/year)	65482.09

Table 15. Simulation results in the 30-bus test case by DE with uncertain loads

index	Expected Value	Std	index	Expected Value
THD (%)	4.753669	1.22	Injected reactive power (MVar)	5.55
Maximum voltage (pu)	1.05	5.3E-05	Energy losses (MWh)	233.03
Minimum voltage (pu)	0.99882	0.00973	Capacitor cost (\$/year)	1023.15
Power losses (MW)	0.451	0.031	Total cost (\$/year)	66794.62

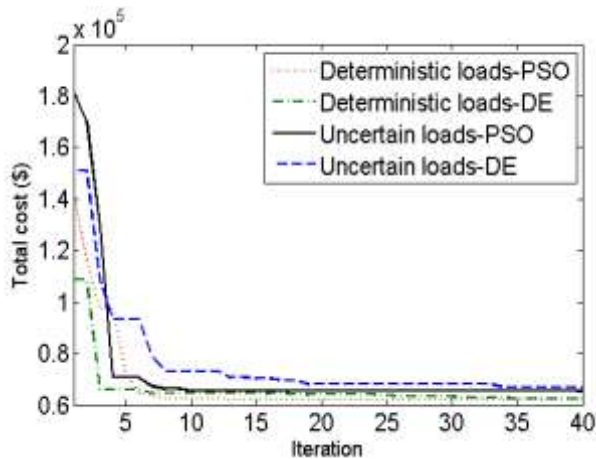


Fig. 10. Convergence diagram of the 30-bus test case

6.6. Sensitivity analysis

Sensitivity analysis has been conducted on the generation levels of wind turbines in order to more comprehension of wind uncertainty behavior.

Table 16. Optimal capacitors set in the 30-bus test case

Reactive power size (MVar)		Q ₁₋₁	Q ₁₋₂	Q ₁₄	Q ₁₆	Q ₂₀	Q ₂₄	Q ₂₆
Deterministic loads	DE	3.3	0.3	0.3	0.3	1.2	0.15	0.45
	PSO	1.2	0.75	2.25	1.8	0	0	0
Uncertain loads	DE	1.8	0	0.45	0.9	2.4	0	0
	PSO	0	1.35	0.15	3.3	0.6	0	0

Situation of harmonics and loads are same as first scenario. As mentioned in section 2-3, wind turbine generations are approximated by different steps. Number of steps affects on accuracy and computational time of the capacitor placement problem. More steps cause more accuracy and more execution time. Therefore, a trade off must be selected between accuracy and time. In this regard, a sensitivity analysis has been done and the results are available in Table 17. Figure 11 also depicts the convergence process. It is obvious that total cost of 6, 8 and 10 generation levels are very close. So, six generation levels will be appropriate for simulation process.

Table 17. Sensitivity analysis on number of wind turbine generation levels

Number of generation level	Expected values				
	Loss (MW)	THD (%)	Maximum voltage (pu)	Minimum voltage (pu)	Total cost (\$/year)
4	0.1847	4.98	1.014	0.977	105545
6	0.1796	4.96	1.010	0.972	102066
8	0.1767	4.99	1.013	0.975	101162
10	0.1752	4.96	1.020	0.983	100189

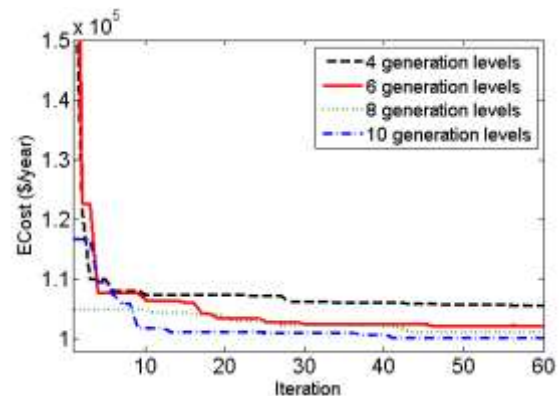


Fig. 11. Convergence diagram of different wind generation levels in 30-bus test case

7. CONCLUSION

Capacitor placement in a probabilistic and harmonic environment is proposed in this paper. Simulations are conducted in different scenarios and generation and load

uncertainties are considered in them. Efficiency of the proposed method is also shown in the presence of the non-linear loads and harmonics with two algorithms. Influence of the generation uncertainties and wind turbine harmonic are investigated in the first and second scenarios. It is demonstrated that the proposed method could only reach to the best solution by changing the combination of capacitors generation in the presence of wind turbine harmonics. Load uncertainties are also considered in the third and the fourth scenarios. The fourth scenario shows the difference of the deterministic and uncertain space. Indeed, uncertainty increases the total cost comparing with the deterministic loads. Efficiency of PHPF is demonstrated using Monte Carlo Simulation. It can be said that PHPF is a capable power flow method and it can be used in the other harmonic and probabilistic problems. Finally, a sensitivity analysis is conducted on the wind turbine generation levels. Their sensitivity is demonstrated by simulation of the different number of generation levels and then, six steps generation levels is considered for simulation process.

REFERENCES

- [1] S. K. Bhattacharya, S. K. Goswami, "A new fuzzy based solution of the capacitor placement problem in radial distribution system", *Expert Syst. Appl.*, vol. 36, pp. 4207-4212, 2009.
- [2] M. Ladjavardi, M. A. S. Masoum, "Genetically optimized fuzzy placement and sizing of capacitor banks in distorted distribution networks", *IEEE Trans. Power Delivery*, vol. 23, pp. 449-456, 2008.
- [3] V. Farahani, S. H. H. Sadeghi, H. A. Abyaneh, S. M. M. Agah, K. Mazlumi, "Energy loss reduction by conductor replacement and capacitor placement in distribution systems", *IEEE Trans. Power Syst.*, vol. 28, pp. 2077-2085, 2013.
- [4] A. A. El-Fergany, "Optimal capacitor allocations using evolutionary algorithms," *IET proc. Gener. Trans. Distrib.*, vol. 7, no. 6, pp. 593-601, 2013.
- [5] D. Kaur, J. Sharma, "Multiperiod shunt capacitor allocation in radial distribution systems," *Int. J. Electric Power Energy Syst.*, vol. 52, pp. 247-253, 2013.
- [6] A. Mendes, P. M. Franca, C. Lyra, C. Pissarra, C. Cavellucci, "Capacitor placement in large-sized radial distribution networks," *IET proc. Gener. Trans. Distrib.*, vol. 152, no. 4, pp. 496-502, 2013.
- [7] Y. Baghzouz, "Effects of nonlinear loads on optimal capacitor placement in radial feeders", *IEEE Trans. Power Delivery*, vol. 6, pp. 245-251, 1991.
- [8] Y. Baghzouz and S. Ertem, "Shunt capacitor sizing for radial distribution feeders with distorted substation voltages", *IEEE Trans. Power Delivery*, vol. 5, pp. 650-657, 1990.
- [9] G. Bei, A. Abur, "Optimal capacitor placement for improving power quality", in *Proc. of the IEEE Power & Energy Society General Meeting*, vol. 1, pp. 488-492, 1998.
- [10] E. Baran, F. Wu, "Optimal capacitor placement in distribution systems", *IEEE Trans. Power Delivery*, vol. 25, pp. 725-734, 1989.
- [11] X. Yan, D. Zhao Yang, W. Kit Po, E. Liu, B. Yue, "Optimal capacitor placement to distribution transformers for power loss reduction in radial distribution systems", *IEEE Trans. Power Syst.*, vol. 28, pp. 4072-4079, 2013.
- [12] S. Nojavan, M. Jalali, K. Zare, "Optimal allocation of capacitors in radial/mesh distribution systems using mixed integer nonlinear programming approach", *Electr. Power Syst. Res.*, vol. 107, pp. 119-124, 2014.
- [13] T. S. Abdel-Salam, A. Y. Chikhani, R. Hackam, "A new technique for loss reduction using compensating capacitors applied to distribution systems with varying load condition," *IEEE Trans. Power Deliver*, vol. 9, pp. 819-827, 1994.
- [14] M. Sedighzadeh, M. M. Mahmoodi, "Optimal reconfiguration and capacitor allocation in radial distribution systems using the hybrid shuffled frog leaping algorithm in the fuzzy framework", *J. Oper. Autom. Power Eng.*, vol. 3, no. 1, pp. 56-70, 2015.
- [15] R. Baghipour, S.M. Hosseini, "A hybrid algorithm for optimal location and sizing of capacitors in the presence of different load models in distribution network", *J. Oper. Autom. Power Eng.*, vol. 2, no. 1, pp. 10-21, 2014.
- [16] S. Sundhararajan, A. Pahwa, "Optimal selection of capacitors for radial distribution systems using a genetic algorithm", *IEEE Trans. Power Syst.*, vol. 9, pp. 1499-1507, 1994.
- [17] T.-L. Huang, Y.-T. Hsiao, C.-H. Chang, J.-A. Jiang, "Optimal placement of capacitors in distribution systems using an immune multi-objective algorithm", *Int. J. Electr. Power Energy Syst.*, vol. 30, pp. 184-192, 2008.
- [18] J.-P. Chiou, C.-F. Chang, C.-T. Su, "Capacitor placement in large-scale distribution systems using variable scaling hybrid differential evolution", *Int. J. Electr. Power Energy Syst.*, vol. 28, pp. 739-745, 2006.
- [19] A. A. El-Fergany, A. Y. Abdelaziz, "Capacitor allocations in radial distribution networks using cuckoo search algorithm," *IET Gener. Transm. Distrib.*, vol. 8, pp. 223-232, 2014.
- [20] A. Seifi, M. R. Hesamzadeh, "A hybrid optimization approach for distribution capacitor allocation considering varying load conditions," *Int. J. Electr. Power Energy Syst.*, vol. 31, pp. 589-595, 2009.
- [21] D. Das, "Optimal placement of capacitors in radial distribution system using a Fuzzy-GA method," *Int. J. Electr. Power Energy Syst.*, vol. 30, pp. 361-367, 2008.
- [22] A. A. El-Fergany, A. Y. Abdelaziz, "Efficient heuristic-based approach for multi-objective capacitor allocation in radial distribution networks," *IET Gener. Transm. Distrib.*, vol. 8, pp. 70-80, 2014.

- [23] A. R. Abul'Wafa, "Reliability/cost evaluation of a wind power delivery system," *Electr. Power Syst. Res.*, vol. 81, pp. 873-879, 2011.
- [24] G. Verbic, C. A. Canizares, "Probabilistic optimal power flow in electricity markets based on a two-point estimate method," *IEEE Trans. Power Syst.*, vol. 21, pp. 1883-1893, 2006.
- [25] S. Chun-Lien, "Probabilistic load-flow computation using point estimate method," *IEEE Trans. Power Syst.*, vol. 20, pp. 1843-1851, 2005.
- [26] R. Billinton, H. Chen, R. Ghajar, "Time-series models for reliability evaluation of power systems including wind energy," *Microelectron. Reliab.*, vol. 36, pp. 1253-1261, 1996.
- [27] R. Billinton, G. Yi, "Multistate wind energy conversion system models for adequacy assessment of generating systems incorporating wind energy," *IEEE Trans. Energy Convers.*, vol. 23, pp. 163-170, 2008.
- [28] R. Karki, R. Billinton, "Cost-effective wind energy utilization for reliable power supply," *IEEE Trans. Energy Convers.*, vol. 19, pp. 435-440, 2004.
- [29] P. Giorsetto and K. F. Utsurogi, "Development of a new procedure for reliability modeling of wind turbine generators," *IEEE Trans. Power Appl. Syst.*, vol. PAS-102, pp. 134-143, 1983.
- [30] D. Xia, G. T. Heydt, "Harmonic power flow studies - part ii implementation and practical application," *IEEE Trans. Power Appl. Syst.*, vol. PAS-101, pp. 1266-1270, 1982.
- [31] M. A. S. Masoum, E. F. Fuchs, "Transformer magnetizing current and iron-core losses in harmonic power flow," *IEEE Trans. Power Delivery*, vol. 9, pp. 10-20, 1994.
- [32] Available online, www.digsilent.de/.
- [33] G. Carpinelli, T. Esposito, P. Varilone, P. Verde, "First-order probabilistic harmonic power flow," in *Proc. of the IEEE Int. Conf. Gener. Trans. Distrib.*, vol. 148, pp. 541-548, 2001.
- [34] A. A. Romero, H. C. Zini, G. Ratta, R. Dib, "Harmonic load-flow approach based on the possibility theory," *IET Gener. Transm. Distrib.*, vol. 5, pp. 393-404, 2011.
- [35] J. Kennedy, R. C. Eberhart, "Particle swarm optimization", in *Proc. of IEEE Int. Conf. Neural Networks*, pp. 1942-1948, 1995.
- [36] D. Zaharie, "Influence of crossover on the behavior of differential evolution algorithms," *Appl. Soft. Comput.*, vol. 9, pp. 1126-1138, 2009.
- [37] W. M. Grady, M. J. Samotyj, A. H. Noyola, "Minimizing network harmonic voltage distortion with an active power line conditioner," *IEEE Trans. Power Delivery*, vol. 6, pp. 1690-1697, 1991.
- [38] M. A. S. Masoum, M. Ladjevardi, A. Jafarian, E. F. Fuchs, "Optimal placement, replacement and sizing of capacitor Banks in distorted distribution networks by genetic algorithms," *IEEE Trans. Power Delivery*, vol. 19, pp. 1794-1801, 2004.
- [39] A. Ulinuha, M.A.S. Masoum, S. Islam, "Hybrid genetic-fuzzy algorithm for volt/var /total harmonic distortion control of distribution systems with high penetration of non-linear loads," *IET Gener. Transm. Distrib.*, vol. 5, pp. 425-439, 2011.
- [40] V. R. Pandi, H. H. Zeineldin, X. Weidong, "Determining optimal location and size of distributed generation resources considering harmonic and protection coordination limits," *IEEE Trans. Power Syst.*, vol. 28, pp. 1245-1254, 2013.